Chapter

A Long-Term Prediction of Beach Changes around River Delta using Contour-Line-Change Model

Takaaki Uda, Shiho Miyahara, Toshiro San-nami and Masumi Serizawa

Abstract

The long-term beach changes along the Kaike coast (Japan) have been investigated. Being a major source of sand to this coast, the Hino River has supplied a large amount of sand during the extensive mining of iron sand in the past, resulting in the shoreline advance. However, the stoppage of the sand mining has caused a marked decrease in the sand supply, resulting in a rapid shoreline recession around the river delta. The beach changes triggered by these human activities have been investigated using an old geographical map and aerial photographs taken between 1947 and 2005. Then, the beach changes have been reproduced using the contour-line-change model considering the change in grain size of the beach sediments. Bathymetric data have been analyzed in order to evaluate the longshore sand transport and the fluvial sand supply from the Hino River. The measured and predicted three-dimensional beach changes were in good agreement and the effectiveness of the contour-line-change model for predicting long-term beach changes was confirmed by this case history.

Keywords: beach changes, contour-line-change model, river delta, longshore sand transport, Kaike coast

1. Introduction

The Yumigahama Peninsula located in the western part of Tottori Prefecture, Japan, has developed as a tombolo owing to the wave-sheltering effect of the Shimane Peninsula with a rich sand supply from the Hino River. The 18-km-long coastline between the Yodoe fishing port and Sakai Port located at both the ends of the peninsula is called the Kaike coast (**Figure 1**). In the Hino River basin, a large-scale mining of iron sand had been carried out in the nineteenth and early twentieth centuries. A huge amount of sand was abandoned in the river basin and such a sand was transported toward the coast through the Hino River. With the cessation of the iron sand mining, however, the sand discharge from the Hino River markedly decreased, causing a strong erosion around the river mouth. The erosion on the Kaike coast was severe from the early 1930s to immediately after World War II. At first, groins were constructed as a measure against erosion, and the construction of detached breakwaters began in 1971. Behind 12 detached breakwaters constructed by 1982, cuspate forelands were well developed [1–3]. Although these detached

Figure 1.
Location of Yumigahama Peninsula in Tottori Prefecture, Japan.

breakwaters and cuspate forelands have been stably maintained, fine-grained sand was locally deposited, natural sandy beaches rapidly disappeared, and the coastline was covered by artificial structures in the entire Yumigahama Peninsula [4].

In predicting the beach changes triggered by the imbalance in longshore sand transport on a coast such as the Kaike coast, a long-term prediction in an extensive area is required [5]. In such a case, the time scale changes from years to decades and the calculation domain reaches even up to 10–100 km. The N-line model can be applicable to the prediction of such beach changes [6–12]. We have developed the contour-line-change model considering the changes in grain size of the seabed materials as a type of N-line model to predict long-term beach changes including the prediction of changes in grain size [13, 14]. The model has applied to the long-term prediction of beach changes around a river mouth delta and those along an arc-shaped shoreline in previous papers.

Uda et al. [15] have first shown a predictive model of the three-dimensional development and deformation of a river mouth delta. This model enabled the prediction of not only the shoreline change but also the three-dimensional, long-term topographic changes around a river mouth, and offshore sand transport can be taken into account when the sea bottom slope exceeds a critical value given by the angle of repose of sand. Furuike et al. [16] have applied the model to the Enshu-nada coast. The shoreline changes between the Magome river mouth and Imagire-guchi jetty have been investigated where beach changes triggered by the decrease in fluvial sand supply from the Tenryu River occur. It was observed that the shoreline retreated downcoast of the Magome river mouth, and the shoreline advanced in parallel further downcoast, while maintaining the curvature in the shoreline configuration. Miyahara et al. [17, 18] have investigated the long-term evolution of the Tenryu River delta associated with sand bypassing at several dams. When the sediment yield from the river was artificially increased, the supplied sediment was mainly deposited around the river mouth, but it took a longer time for a sandy beach far from the river mouth to recover. Given the annual discharge of sediment with three grain sizes, the recovery of the delta topography and the effect of nourishment on the nearby coast have been predicted. San-nami et al. [19] have analyzed the beach changes of Kujukuri Beach with a 60 km length located in Boso Peninsula. On south Kujukuri Beach, severe beach erosion has occurred since the

1970s, and the erosion area has been expanding. The exhaustion of sand supply by northward longshore sand transport from the sea cliffs, formation of a wave-shelter zone at Katakai fishing port breakwater, and ground subsidence caused by the pumping-up of underground water were the major causes of the shoreline recession. The arc-shaped shoreline of Kujukuri Beach was reproduced given these conditions. Furthermore, San-nami et al. [20] have investigated the long-term topographic changes since 1968 along the entire Shizuoka and Shimizu coasts including a 17 km stretch extending between the Abe River and the Mihonomatsubara sand spit. The beach erosion of these coasts was triggered by the decrease in sediment supply from the Abe River due to excessive riverbed mining until 1967. After 1982/1983, the natural sand supply from the river increased and accretion occurred on these coasts. Measured topographic changes were reproduced using the model. Not only the movement of the sand body but also the shoreline and bathymetric changes were numerically reproduced.

Upon these previous studies, the long-term topographic changes of the Kaike coast in a 70-year period have been analyzed in this study, including the period when extensive mining of iron sand has been carried out. Then, given these conditions, the process of the reduction in the size of the Hino River delta over 70 years was reproduced using the contour-line-change model considering the change in grain size of the seabed material, and the applicability of the model was validated.

2. Long-term shoreline changes along Yumigahama Peninsula and longshore sand transport

2.1 Shoreline changes

The shoreline configurations in the Yumigahama Peninsula were determined from an old geographical map produced in 1899 and the aerial photographs taken in 1947, 1967, and 1973. The shoreline changes in 74 years were investigated between 1899, when rich sediment was supplied from the Hino River during the period of iron sand mining, and 1973, when the construction of detached breakwaters began. In the analysis of the shoreline changes, the correction owing to the changes in tide level was made using the tide level when the aerial photograph was taken and the mean foreshore slope of 1/15. The origin of the coordinate (x = 0 km) was set at the left bank of the Hino River and the alongshore distance x was taken westward along the coastline (**Figure 1**).

Figure 2 shows the shoreline changes between 1899 and 1947. The shoreline markedly retreated in an area between x = 1 and $-x$ = 2 km around the Hino River mouth with the decline of mining of iron sand, and the shoreline receded by a maximum of 250 m at the river mouth. On the other hand, in the areas westwards and eastwards of x = 3 km, the shoreline advanced of 100 m in parallel at a rate of 2 m/year, except that in the vicinity of Yodoe fishing port. Similarly, **Figure 3** shows the shoreline changes with reference to shoreline in 1947 until 1967 and 1973, after that two detached breakwaters were constructed. Since a seawall and groins have been constructed in an area between x = 0 and x = 1.5 km westwards of the Hino River until 1967, the shoreline recession was prevented. However, excluding this area, the shoreline retreated westwards of the protected area. The eroded sand was transported westwards of x = 5 km, resulting in the shoreline advance. Until 1973, the area where the shoreline markedly receded expanded westwards, and the area where the shoreline advanced until 1967 was eroded. Here, the shoreline advance at two locations near x = 1 km was due to the formation of cuspate forelands behind the detached breakwaters constructed by 1973.

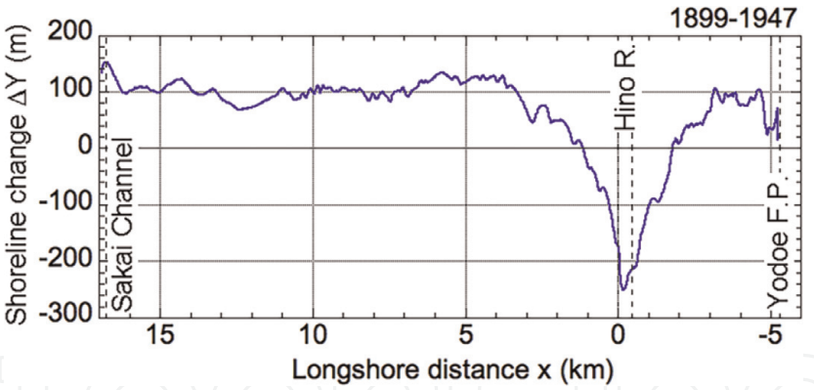

Figure 2.
Shoreline changes in entire Yumigahama Peninsula (reference year: 1899).

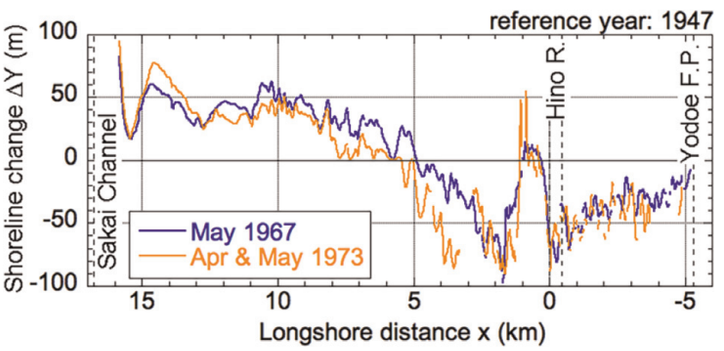

Figure 3.
Shoreline changes until 1967 and 1973 in entire Yumigahama Peninsula (reference year: 1947).

2.2 Analysis of bathymetric survey data

Using the bathymetric survey data (200 m intervals), the bathymetry in 2000 and the bathymetric changes between 1980 and 2000 have been represented (**Figures 4** and **5**). The eroded and accreted sand volumetric changes relative to those occurring in 1980 are also shown together with the locations of the detached breakwaters (DBs; **Figure 5**). The contours shallower than −8 m markedly protruded near the river mouth delta, and the DBs were constructed immediately westwards of this river delta. Twelve DBs were constructed from 1971 to 1982. With the construction of DBs, sand was deposited behind these breakwaters, whereas erosion occurred in the offshore zone between −4 and − 7 m, and down the coast of the accretion area. These beach changes were considered to be due to the blocking of westward alongshore sand transport by the DBs.

2.3 Longitudinal profiles and depth change in median diameter

In July 2002, the sampling of the seabed material was carried out in the depth zone between +3 and − 12 m along transect x = 1.3 km at 1-m-depth intervals. **Figure 6** shows the longitudinal profile and depth distribution of median diameter (d_{50}) along this transect. Coarse sand of d_{50} ranging from 0.3 to 0.7 mm is deposited on the foreshore, and d_{50} decreases with increasing depth, and well-sorted fine sand with a grain size of 0.13 mm is deposited in the depth zone deeper than −8 m. Corresponding to this grain size distribution, the seabed slope is as steep as 1/6 on the foreshore, 1/30 between −2 and − 8 m, and a very gentle slope of 1/100 in the depth zone deeper than −8 m. From these data, it is found that the depth of closure (h_c) is approximately 8 m on this coast, and the seabed near h_c is covered by fine

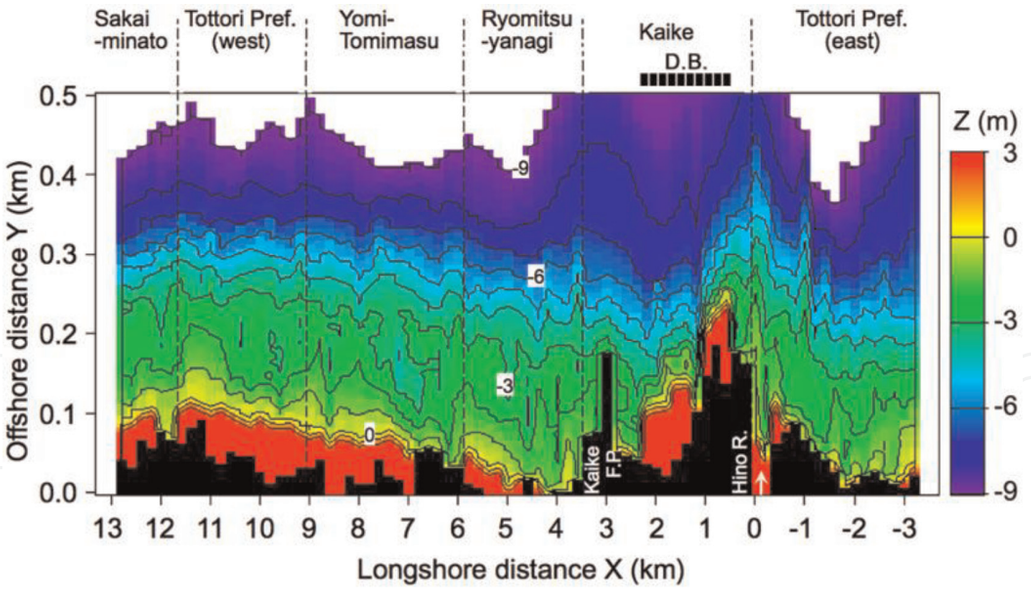

Figure 4.
Bathymetry in 1980 using expanded coordinates.

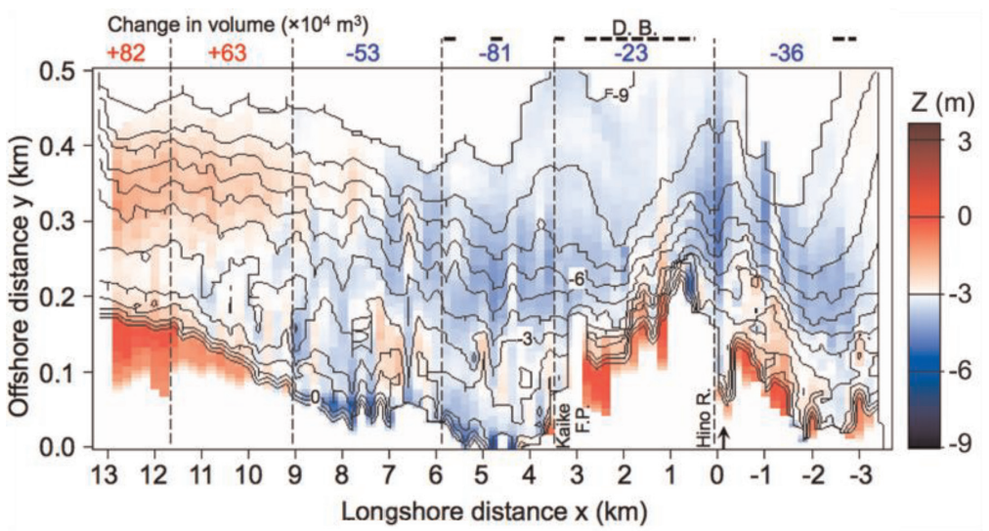

Figure 5.
Bathymetry in 2000 using expanded coordinates and bathymetric changes with reference to that in 1980.

sand. The depth distribution of d_{50} can be separated into three subregions, as shown in **Figure 6**, with longitudinal slopes of 1/6, 1/30, and 1/100, i.e., fluvial sediment supplied from the Hino River is mainly distributed in the depth zone corresponding to the grain size of the material, and coarser material is deposited near the shoreline, and the component finer than the grain size of 0.13 mm is deposited in the zone deeper than −8 m. In addition, fine sand of d_{50} = 0.3 mm is deposited in the intermediate depth zone between −2 and − 8 m. Although westward longshore sand transport prevails on the coast, sand is transported along the depth zones separated in two layers associated with the grain size sorting (**Figure 6**). Thus, the changes in contour lines in the depth zones I and II between z = +3 and − 2 m and between z = −2 and − 8 m could be separately calculated, where the average grain sizes are 0.5 and 0.3 mm, respectively.

Figure 7 shows the longshore distribution of changes in sand volume in the depth zones I and II between 1980 and 2009. In the depth zone I, the sand volume was almost constant east of x = 5 km except for the local deposition of sand behind

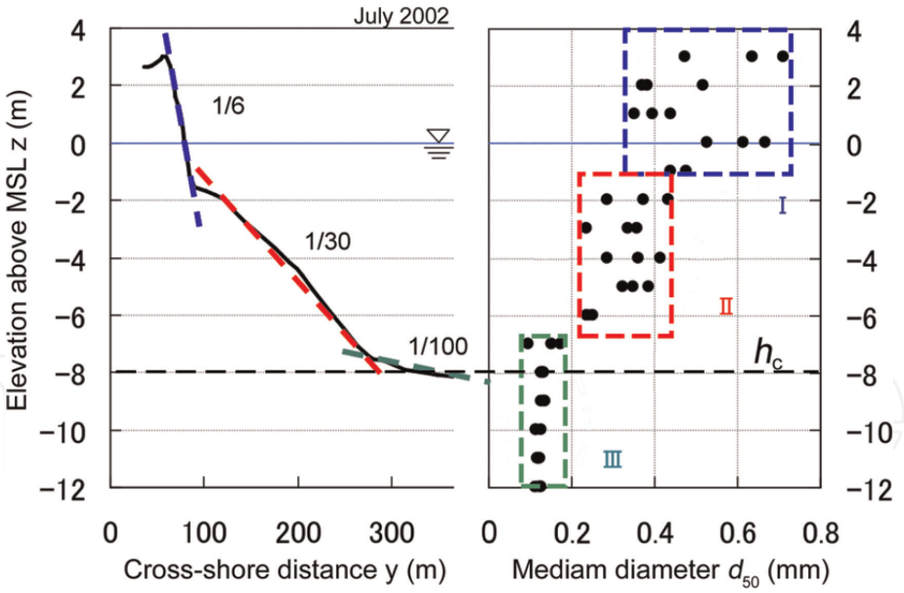

Figure 6.
Longitudinal profile along transect x = 1.3 km and depth distribution of d_{50} measured in July 2002.

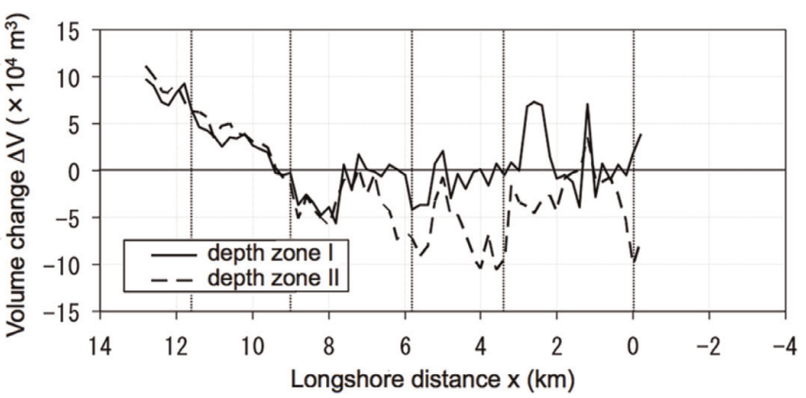

Figure 7.
Longshore distribution of changes in sand volume in depth zones I and II between 1980 and 2009.

detached breakwaters constructed between x = 0 and 4 km, and the accreted sand volume was 1.34 × 10^6 m^3 in contrast to the eroded sand volume of 5.8 × 10^5 m^3. The sand volume in the depth zone II decreased between x = 2 and 9 km, whereas it increased west of x = 9 km; the eroded volume was 2.01 × 10^6 m^3 greater than the accreted volume of 1.06 × 10^6 m^3. However, the eroded and accreted sand volumes in the entire depth zones I and II were 2.59 × 10^6 and 2.40 × 10^6 m^3, respectively, and the accreted volume accounts for 93% of the eroded volume.

2.4 Longshore sand transport

The west and east ends of the study area are the solid boundaries of the reclaimed land and Yodoe fishing port; thus, the distribution of longshore sand transport can be calculated by integrating the shoreline change from these boundaries to the Hino River mouth, and multiplying by the characteristic height of beach changes, which is defined by the correlation coefficient between the change in the cross-sectional area of the beach and the shoreline change, and then divided by the elapsed time. Since the relationship of h = (1.0∼1.3)h_c holds between the characteristic height of beach changes (h) and h_c [4], and h_c on this coast is approximately equal to 8 m, h becomes 10 m.

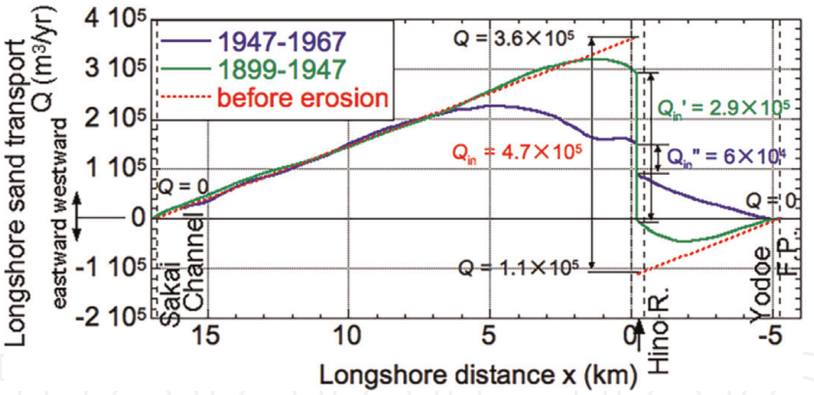

Figure 8.
Distribution of longshore sand transport between 1899 and 1947 and between 1947 and 1967.

Figure 8 shows the distribution of longshore sand transport between 1899 and 1947, and between 1947 and 1967 with a positive sign for westward longshore sand transport. Although westward and eastward longshore sand transports took place on the west and east sides of the river mouth between 1899 and 1947, respectively, the distribution of longshore sand transport changes linearly with the same slope west of $x = 3$ km and east of $x = -3$ km, and they smoothly converge to the distribution between 1947 and 1967 west of $x = 7$ km. Westward and eastward longshore sand transports take maximum rates of 3.2×10^5 and 4.6×10^4 m^3/year at $x = 1$ and -1.8 km, respectively. On both sides of these points, the longshore sand transport is linearly distributed, so that it is found that the shoreline has advanced in parallel over time except for the erosion area close to the river delta. The longshore sand transport has a difference of 2.9×10^5 m^3/year between both sides of the river mouth, implying that the same amount of sand was supplied from the river during the period. In contrast, longshore sand transport became westward in the entire area between 1947 and 1967 after the fluvial sand supply was markedly reduced owing to the stoppage of the mining of iron sand with a maximum rate of 2.3×10^5 m^3/year at $x = 5$ km. The location where the longshore sand transport takes a peak value shifted westward compared with that between 1899 and 1967, implying that the erosion area expanded westward. Furthermore, since longshore sand transport on the west and east sides of the river mouth become 1.5×10^5 and 9.0×10^4 m^3/year, respectively, sediment inflow from the river results in 6.0×10^4 m^3/year. In addition, in **Figure 8**, the longshore sand transport linearly increased from the west end to a location of $x = 7$ km in both periods between 1899 and 1947 and between 1947 and 1967, and the effect of the decrease in the longshore sand transport did not reach far from the river mouth, resulting in the parallel advance of the shoreline. Therefore, when this straight line is extrapolated toward the river mouth, a straight line indicated by "before erosion" in **Figure 8** is obtained, and the longshore sand transport at the river mouth became 3.6×10^5 m^3/year, which is assumed to be the westward longshore sand transport before the initiation of erosion.

In the area east of the river mouth, eastward longshore sand transport could have prevailed with the development of the river delta, and the longshore sand transport is assumed to have a linear distribution with the same longshore inclination as that west of the river mouth to satisfy the conditions that the shoreline around the river mouth is continuous and the river delta parallelly advanced in the offshore direction. By extrapolating a straight line with the same inclination as that west of the river mouth from Yodoe fishing port, we obtained a longshore sand transport of 1.1×10^5 m^3/year on the east side of the river mouth. Finally, the entire sediment supply from the river in the period when iron sand was mined is assumed

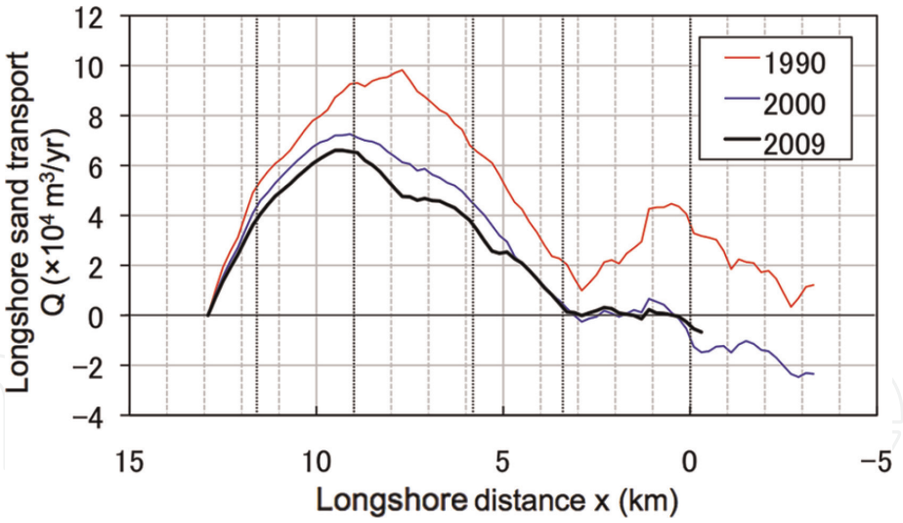

Figure 9.
Distribution of longshore sand transport calculated from beach changes between 1980 and 2009.

to be 4.7×10^5 m^3/year as the sum of longshore sand transport on both sides of the river mouth. In addition, since the longshore inclination of longshore sand transport in **Figure 8** gives 21 m^3/m/year as the rate of sand accretion, the rate of the advance of the river delta becomes 2.1 m/year, when dividing this rate by the characteristic height of beach changes of h = 10 m.

Similarly, the distribution of longshore sand transport after 1980 was evaluated by integrating the topographic changes between 1980 and 2009 in the east from the west end, and dividing by the elapsed time. **Figure 9** shows the results. The longshore sand transport took a maximum of 1.0×10^5 m^3/year at x = 7.5 km in 1990 with a secondary peak at x = 0 km. After 2000, it has decreased in the eastern part, and it took a maximum of 6.5×10^4 m^3/year in 2009.

3. Change in apex angle of Hino River delta and predominant wave direction

Figure 10 shows the geographical map in 1899 and aerial photograph in 1947. The apex angle of the river delta (angle AOB) in 1899 was 170°. Assuming that the wave crest line of the predominant wave incident to the river delta is given by a straight line of A′OB′ in **Figure 10(a)**, the breaker angles between the shoreline on both sides of the river delta and the wave crest line are given by AOA′ and BOB′. These breaker angles can be evaluated as follows. First, the sum of these breaker angles becomes 10° by subtracting the apex angle of the river delta of 170° from 180°. In the distribution of the longshore sand transport shown in **Figure 8**, the longshore sand transport on the west and east sides of the Hino River mouth are 3.6×10^5 and 1.1×10^5 m^3/year, respectively, resulting in the ratio of longshore sand transport on both sides of 3:1, because the longshore sand transport is proportional to the breaker angle. Taking these conditions into account, the breaker angles on the left and right banks of the river mouth decrease to 7.5° and 2.5°, respectively, when separating 10° by the ratio of 3:1. Finally, the predominant wave direction normal to A′B′ is assumed to be N13°E.

In 1947, the shoreline of the river delta receded because of the decrease in sand supply from the river, as shown in **Figure 10(b)**, and the apex angle increased to up to 175°, and the breaker angles on the left and right banks of the river became 5° and 0°, respectively, taking the predominant wave direction of N13°E calculated as

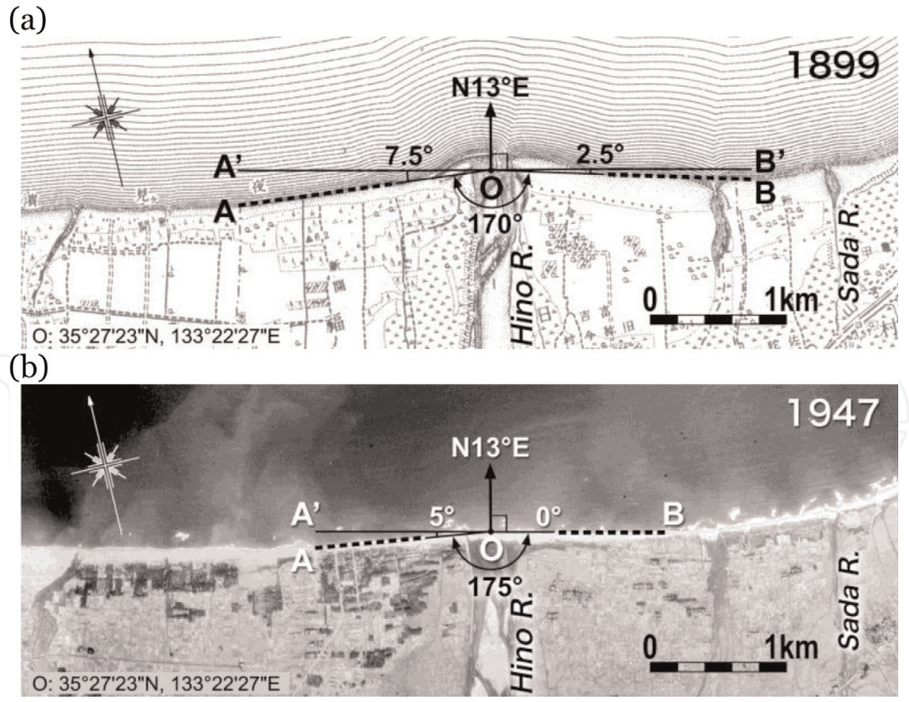

Figure 10.
Change in apex angle of Hino River delta and predominant wave direction. (a) 1899. (b) 1947.

mentioned above. The decrease in the breaker angle west of the river mouth corresponds to the decrease in the westward longshore sand transport.

4. Contour-line-change model considering change in grain size

A numerical model described in [13, 14] was used. Let the x- and z-axes be the longshore distance and seabed elevation relative to the still water level, respectively, and $Y(x, z, t)$ is the offshore distance to a specific contour line to be solved. To consider the sorting of sand of different grain sizes by cross-shore sand transport, the depth distribution of cross-shore sand transport considering the grain size effect in mixing was considered. The sorting of grain size populations was modeled by introducing the equilibrium slope angle $\beta_c{}^{(k)}$, which corresponds to each grain size population k. In this case, a grain size population was assumed to have a single equilibrium beach slope with a characteristic grain size $d^{(k)}$. By assuming that the mobility of sand of each grain size population by cross-shore movement is the same as that of longshore sand transport, the coefficient of the sediment transport rate according to the grain size $d^{(k)}$, which was given in [21, 22], was introduced. Furthermore, assuming that the ratio of the exposed area of each grain size population to the entire sea bottom area is equal to the content of each size population in the exchange layer $\mu^{(k)}(k = 1, 2, \cdots, N)$, the cross-shore sand transport of each grain size population $q_z{}^{(k)}$ is derived.

Cross-shore sand transport:

$$q_z^{(k)} = \mu^{(k)} \cdot \varepsilon_z(z) \cdot \gamma \cdot K_1^{(k)} \cdot \left(EC_g\right)_b \cos^2\alpha_b \sin\overline{\beta} \cdot \left(\cot\beta / \cot\beta_c^{(k)} - 1\right); \quad k = 1, 2, \cdots, N \tag{1}$$

$$K_1^{(k)} = \frac{A}{\sqrt{d^{(k)}}}; k = 1, 2, \cdots, N \tag{2}$$

$$\cot\beta = -\partial Y/\partial z \tag{3}$$

$$\varepsilon_x(z) = \begin{cases} \left(2/h_c^3\right)(h_c/2 - z)(z + h_c)^2, & -h_c \le z \le h_R \\ 0, z \le -h_c, z \ge h_R \end{cases} \tag{4}$$

Here, $q_z^{(k)}(k = 1, 2, \cdots, N)$ is the cross-shore sand transport per unit length in the longshore direction for each grain size population, $\mu^{(k)}$ is the content of each grain size population (k) in the exchange layer of sand, $(EC_g)_b$ is the wave energy flux at the breaking point, $K_1{}^{(k)}$ is the coefficient of longshore sand transport, $\varepsilon_z(z)$ is assumed to be equivalent to the depth distribution of the longshore sand transport $\varepsilon_x(z)$ given by Uda and Kawano [23], and $d^{(k)}$ is a typical grain size of the grain size population. A is a coefficient that depends on the physical conditions of the beach. $d^{(k)}$ in Eq. (2) has a unit of mm. γ is the ratio of the coefficient of cross-shore sand transport to that of longshore sand transport ($\gamma = K_z{}^{(k)}/K_1{}^{(k)}$) and expresses the mobility of cross-shore sand transport relative to that of longshore sand transport, α_b is the angle between the wave crest line at the breaking point and each contour line, and β is the beach slope angle at each contour line. $\overline{\beta}$ is the average beach slope angle between the berm height h_R and the depth of closure h_c, and $\beta_c{}^{(k)}$ is the equilibrium beach slope angle. When the beach slope becomes steeper than the angle of repose of sand, sand is transported offshore by gravity. By this procedure, we can calculate the formation of a scarp in a zone larger than h_R and the sinking of sand in a zone larger than h_c.

Longshore sand transport:

$$q_x{}^{(k)} = \mu^{(k)} \cdot \varepsilon_x(z) \cdot K_1^{(k)} \cdot \left(EC_g\right)_b \cdot \left(\cos\alpha_b \sin\alpha_b - \xi \frac{1}{\tan\beta_b} \cdot \cos\alpha_b \cdot \frac{\partial H_b}{\partial x} \right); \tag{5}$$

$$k = 1, 2, \cdots, N$$

Here, $q_x^{(k)}(k = 1, 2, \cdots, N)$ is the longshore sand transport per unit depth for each grain size population, $\square\varepsilon_x(z)$ is the depth distribution of longshore sand transport, and ξ is the constant given by $K_2{}^{(k)}/K_1{}^{(k)}$, which depends on the physical conditions of the beach, where $K_2{}^{(k)}$ is a function of $K_1{}^{(k)}$ and is equivalent to the coefficient of Ozasa and Brampton [24]. $\tan\beta_b$ is the beach slope in the surf zone and H_b is the breaker height.

Mass conservation for each grain size:

$$\frac{\partial y^{(k)}}{\partial t} = -\frac{\partial q_x^{(k)}}{\partial x} - \frac{\partial q_z^{(k)}}{\partial z} + S^{(k)}; \tag{6}$$

$$k = 1, 2, \cdots, N$$

Here, $S^{(k)}(k = 1, 2, \cdots, N)$ is the additional term for calculating the sand source for each grain size population, by which sediment supply from a river or the sand supply by beach nourishment is given. The total contour-line change at a certain position is determined by the summation of the contour-line changes of all grain size populations at that position.

$$\frac{\partial Y}{\partial t} = \sum_{k=1}^{N} \frac{\partial y^{(k)}}{\partial t} \tag{7}$$

Change in content of each grain size population:

$$\frac{\partial \mu^{(k)}}{\partial t} = \frac{1}{B}\left\{\frac{\partial y^{(k)}}{\partial t} - \frac{\partial Y}{\partial t}\cdot \mu^{(k)}\right\},\ \frac{\partial Y}{\partial t} \geq 0; \quad k = 1, 2, \cdots, N \tag{8}$$

The content of each grain size population in the new exchange layer formed during erosion is expressed as:

$$\frac{\partial \mu^{(k)}}{\partial t} = \frac{1}{B}\left\{\frac{\partial y^{(k)}}{\partial t} - \frac{\partial Y}{\partial t}\cdot \mu_B^{(k)}\right\},\ \frac{\partial Y}{\partial t} \leq 0; \quad k = 1, 2, \cdots, N \tag{9}$$

where $\mu_B^{(k)}$ is the content of each grain size population on the sandy beach landward of the initial exchange layer. The width B of the exchange layer is determined with reference to the mixing depth reported by Kraus [25]. The abovementioned equations were solved simultaneously. In the numerical simulation, the calculation points of the contour-line position and sand transport rate are set in staggered meshes with a difference of 1/2 mesh; the cross-shore and longshore sand transport are calculated using Eqs. (1) and (5), respectively. In this case, the upcoast value depending on the direction of sand transport is employed as $\mu^{(k)}$ in Eqs. (1) and (5). The bathymetric changes can be calculated using Eqs. (6) and (7). $\mu^{(k)}$ is calculated using Eqs. (8) and (9), and the calculation point of $\mu^{(k)}$ is set at the same point for calculating the contour-line position.

5. Reproduction of reduction in size of Hino River delta

5.1 Calculation conditions

The numerical simulation of topographic changes relative to the initial topography in 1899 was carried out until 1967, when a large amount of sand was supplied from the river as a result of the extensive mining of iron sand, and then sand supply (Q_{in}) markedly decreased after the stoppage of the mining. The calculation period was separated into four periods corresponding to the sand discharge and the structural conditions of the coast. In the first period between 1899 and 1920, Q_{in} of 4.7×10^5 m^3/year was supplied from the river, resulting in the development of the river delta. In this period, the shoreline in the entire area advanced at a rate of 2 m/year, and the entire shoreline advance reached 42 m by 1920.

In the second period between 1920 and 1947, Q_{in} began to decrease from 4.7×10^5 m^3/year before 1920 to 1.5×10^5 m^3/year after 1920. Q_{in} of 1.5×10^5 m^3/year was calculated by subtracting the sand volume in the first period (4.7×10^5 m^3/year $\times$ 21 year) from that between 1899 and 1947 (2.9×10^5 m^3/year $\times$ 48 year), which was determined from the shoreline changes between 1899 and 1947, and divided by the elapsed time of 27 years. In the third period between 1947 and 1962, Q_{in} decreased until 6×10^4 m^3/year owing to the stoppage of mining of iron sand, which was calculated from the measured shoreline changes between 1947 and 1967. In the fourth period between 1962 and 1967, the seawall and groins were constructed west of the Hino River mouth, although Q_{in} remained constant at 6×10^4 m^3/year.

By setting the coastline lengths in the areas west and east of the river mouth to be L_1 and L_2, we found that the wave directions $-\theta_1$ and θ_2 immediately west and east of the river mouth, respectively, satisfy a relationship of $-\theta_1/\theta_2 = L_1/L_2 = 3$. In

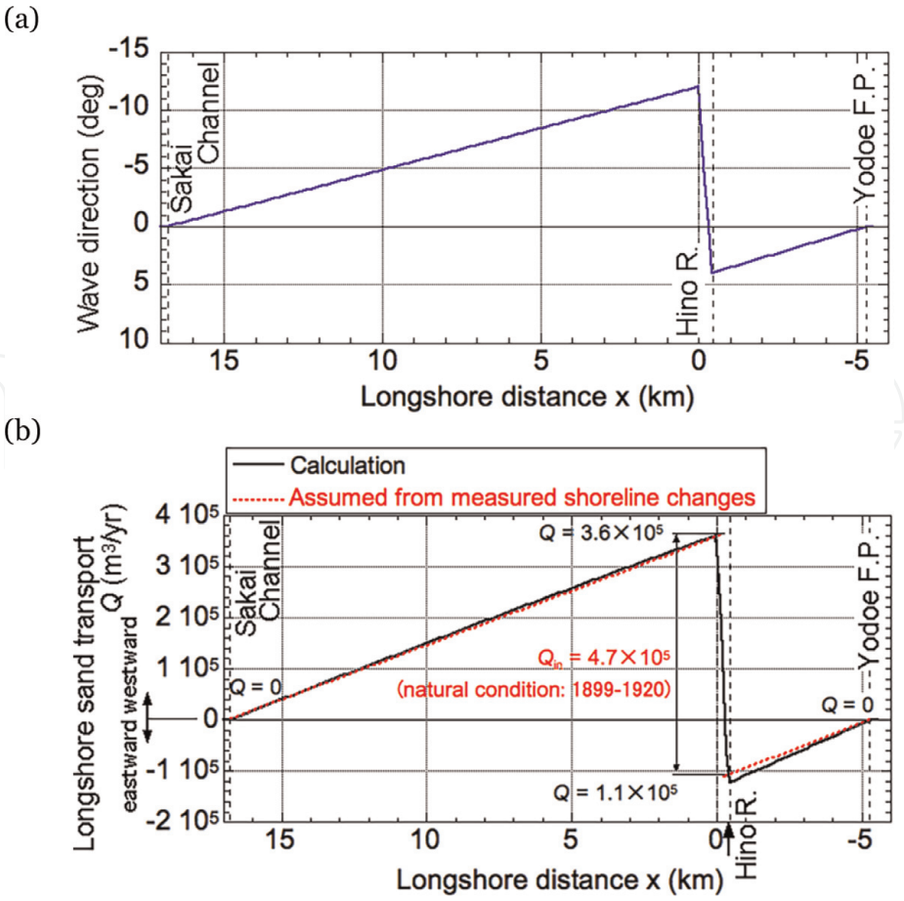

Figure 11.
Wave direction and distribution of longshore sand transport used for calculation. (a) Wave direction. (b) Longshore sand transport.

addition, $-\theta_1$ and θ_2 are approximately given by 7.5° and 2.5°, respectively, from the geographical map in 1899, as shown in **Figure 10**. Thus, after the trial-and-error calculation of the shoreline changes, while satisfying the relation of $\theta_1/\theta_2 = 3$, we obtained $-\theta_1 = 12°$ and $\theta_2 = 4°$ for the best fit results. Finally, a linear distribution shown in **Figure 11(a)** was assumed with angles of −12° and 4° immediately west and east of the Hino River mouth, respectively. **Figure 11(b)** shows the distribution of longshore sand transport at the initial stage. For the wave condition, the breaker height was determined as $H_b = 1.1$ m on the basis of the energy mean significant wave height measured between 1995 and 2008 at Hiezu wave observatory.

The initial seabed slope was assumed to be 1/6 between $z = +3$ and -2 m, and 1/30 between $z = -2$ and -8 m. The number of grain sizes (N) was set to 2 with characteristic grain sizes of $d^{(1)} = 0.3$ mm for fine sand and $d^{(2)} = 0.5$ mm for coarse sand. The initial contents μ_1 and μ_2 for fine and coarse sand were, respectively, assumed to be 0.0 and 1.0 in the cell between $z = +3$ and -1 m, 0.5 and 0.5 in the cell at $z = -2$ m, and 1.0 and 0.0 in the cell between $z = -3$ and -8 m. The equilibrium slopes $\tan\beta_c^{(1)}$ and $\tan\beta_c^{(2)}$ of fine and coarse sand were, respectively, assumed to be 1/30 and 1/6, on the basis of the measured longitudinal profile. As for the sand back pass on the coast, sand was extracted from the foreshore with an elevation between 0 and + 3 m at $x = 13$ km, and the same amount of sand was supplied from the foreshore at $x = 8$ km. **Table 1** summarizes the other calculation conditions.

5.2 Results of numerical simulation

Figure 12 shows the bathymetric changes from the first to the fourth periods together with an additional expression of bathymetric changes relative to the

Calculation method	**Contour-line-change model considering grain size changes**
Calculation domain	Sakai channel to Yodoe fishing port
Q_{in} in each calculation period	Reproduction calculation between 1899 and 1967 1 (1899–1920): 4.7×10^5 m^3/year 2 (1920–1947): 1.5×10^5 m^3/year 3 (1947–1962): 6×10^4 m^3/year 4 (1962–1967): 6×10^4 m^3/year + seawall
Initial bathymetry	Straight parallel contours between z = +3 m and − 2 m with 1/6 slope, between z = −2 m and − 8 m, 1/30 slope
Grain size	• N = 2 • For characteristic grain sizes, fine sand of $d^{(1)}$ = 0.3 mm coarse sand of $d^{(2)}$ = 0.5 mm • Initial contents z = 3 m to −1 m: μ_1 = 0.0 (fine sand) and μ_2 = 1.0 (coarse sand) z = −2 m: μ_1 = 0.5 (fine sand) and μ_2 = 0.5 (coarse sand) z = −3 m to −8 m: μ_1 = 1.0 (fine sand) and μ_2 = 0.0 (coarse sand)
Equilibrium slope	$\tan\beta_c^{(1)}$ = 1/30 and $\tan\beta_c^{(2)}$ = 1/6
Width of exchange layer	B = 6 m (thickness of exchange layer = 1 m)
Incident wave condition	• Breaker height: H_b = 1.1 m, energy-mean significant wave height measured between 1995 and 2008 at Hiezu observatory • Initial breaker angle: linear distribution between 0° (Sakai channel) and − 12° (Hino River mouth), and between 4° (Hino River mouth) and 0° (Yodoe fishing port)
Tide condition	MSL
Depth of closure and berm height	Depth of closure h_c = 8 m Berm height h_R = 3 m
Coefficient of sand transport	Coefficient of longshore sand transport A = 0.12 for initial longshore sand transport to be $Q = 3.6 \times 10^5$ m^3/year Ratio of cross-shore and longshore sand transports γ = 0.1 Coefficient of Ozasa and Brampton's [18] term ξ = 3.24
Depth distribution of longshore and cross-shore sand transport	Uniform
Critical slope of falling sand	On land: 1/2 and on seabed: 1/2
Calculation range of depth	z = +3.5 to −8.5 m
Mesh sizes	Δx = 100 m (longshore direction) and Δz = 1 m (vertical direction)
Time intervals	Δt = 1 h
Boundary conditions	Left and right boundaries: q_x = 0 Landward and offshore boundaries: q_z = 0

Table 1.
Calculation conditions.

bathymetry in 1920 (**Figure A1**). During the first period, the parallel contours in 1899 simply advanced by 42 m until 1920, so that a new coordinate was taken for the shoreline to be shifted by 42 m seaward. During the second period, a V-shape shoreline recession began around the river mouth because of the decrease in Q_{in} from 4.7×10^5 m^3/year before 1920 to 1.5×10^5 m^3/year. However, the contour lines far

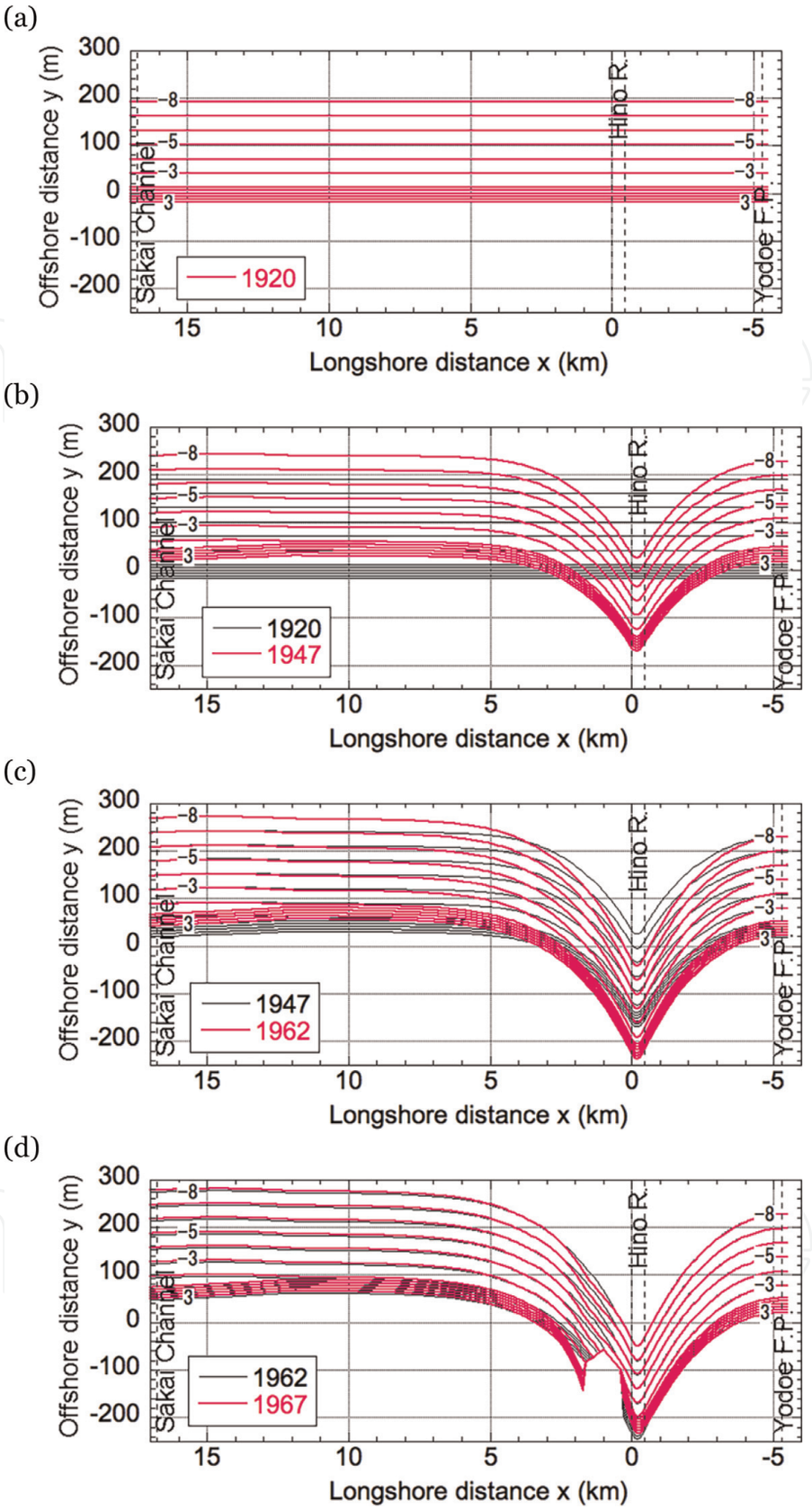

Figure 12.
Bathymetric changes from the first to fourth periods. (a) First period (1899–1920). (b) Second period (1920–1947). (c) Third period (1947–1962). (d) Fourth period (1962–1967).

from the river mouth continued to advance because of the successive supply of sand to both sides of the river mouth. During the third period, the shoreline markedly receded around the river mouth because of the further decrease in Q_{in} from 1.5×10^5 to 6×10^4 m^3/year owing to the stoppage of mining of iron sand. Even during this

period, however, the contour lines continued to advance far from the river mouth. During the fourth period, a seawall was constructed west of the river mouth blocking westward longshore sand transport partially, so that the contour lines receded west of the seawall, even if Q_{in} was maintained at 6×10^4 m^3/year.

The shoreline changes in the entire period relative to that in 1920 can be drawn, as shown in **Figure 13**. The shoreline advanced by 42 m between 1899 and 1920 because of the accretion of the entire river delta. After 1920, however, the shoreline receded around the river delta owing to the decrease in sand supply, whereas the shoreline continued to advance far from the river mouth.

Figure 14 shows the measured and predicted shoreline changes with reference to the shoreline in 1899 and 1947. Regarding the shoreline changes until 1947, the

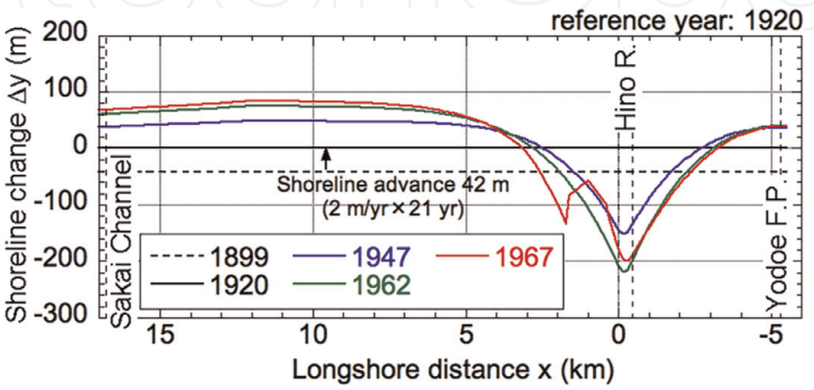

Figure 13.
Shoreline changes with reference to that in 1920.

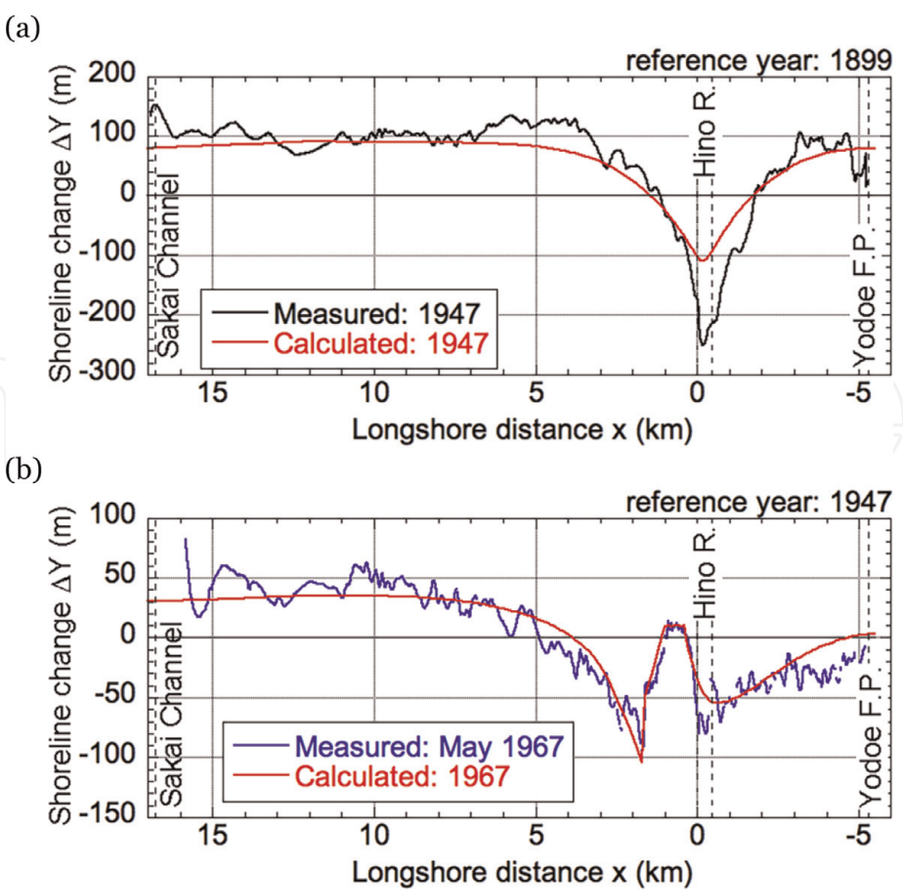

Figure 14.
Measured and predicted shoreline changes between 1899 and 1947 and between 1947 and 1967. (a) 1899–1947. (b) 1947–1967.

overall shoreline changes were reproduced well, except for the river mouth area where the shoreline change was underestimated. Regarding the shoreline changes until 1967, the shoreline changes in the overall area including the shoreline recession west of the seawall constructed immediately west of the river mouth were well reproduced. The predicted and measured shoreline changes are in good agreement.

6. Reproduction of topographic changes relative to topography in 1947

6.1 Calculation conditions

The calculation domain is the same as that in the previous section. In the calculation, the entire period between 1947 and 2010 was separated into five periods, and Q_{in} in each period was calculated from the volumetric change transformed from the shoreline changes measured during the period by multiplying the characteristic height of beach changes. In the first and second periods until 1962 and 1967, respectively, Q_{in} was given as 6×10^4, and 4.7×10^4 m^3/year in the third, fourth, and fifth periods between 1967 and 2010 with a decrease in Q_{in} by 20% after 1967.

For the initial topography, the results of the reproduction calculation until 1947 were employed, assuming parallel contour lines on the expanded coordinates. In the

Q_{in}	1 (1947–1962): 6×10^4 m^3/year 2 (1962–1967): 6×10^4 m^3/year, seawall between x = 0 and 1.5 km 3 (1967–1980): 4.7×10^4 m^3/year, detached breakwater Kaike fishing port, and seawall between x = 0 and − 3.5 km 4 (1980–1995): 4.7×10^4 m^3/year, detached breakwater between x = −3.5 and − 2.5 km, and between 3.5 and − 7 km, seawall between x = −5 and 0 km, and between x = 3.5 and 13 km 5 (1995–2010): 4.7×10^4 m^3/year, sand back pass of 3×10^4 m^3/year, in which sand is subtracted at x = 13 km and nourished at x = 8 km, L-shape groin between x = 7 and − 8 km, artificial reef and detached breakwater between x = −5 and 0 km
Incident wave angle	Initial breaker angle in 1899 minus inclination angle of shoreline reproduced in 1947
Coefficient of sand transport	Coefficient of Ozasa and Brampton's [18] term ξ = 3.24
Remarks	■ Fluvial sand supply from Hino River: sand source distributed in depth zone between z = +3 and − 8 m ■ Sand back pass by a rate of 3×10^4 m^3/year was given by a sink and source of sand between z = 0 and + 3 m ■ Wave transmission coefficient K_t = 0.2 (detached breakwater) except K_t = 0.4 between x = −1.4 and − 0.5 km ■ Artificial reef K_t = 0.8 ■ Port breakwaters at Yodoe and Kaike fishing ports and Sakaiminato Marina K_t = 0.0 ■ Coefficient of Ozasa and Brampton's [18] term ξ = 1.62: detached breakwaters between x = −1.4 and − 0.5 km

Table 2.
Calculation conditions.

calculation, the changes in contour lines between +3 and − 8 m were calculated, assuming the same seabed slopes of 1/6 between z = +3 and − 2 m, and 1/30 between z = −2 and − 8 m. The number of grain sizes (N), the grain sizes of fine and coarse sand, the initial contents of each grain size of μ_1 and μ_2, the equilibrium slope corresponding to each grain size, and the wave conditions are the same as those in the reproduction calculation. The longshore distribution of the initial breaker angle was given by subtracting the inclination angle of the shoreline reproduced in 1947 from the initial breaker angle in 1899. The change in wave field by the construction of structures was calculated using the angular spreading method for irregular waves. The wave transmission coefficient of detached breakwaters was set to K_t = 0.2 as shown in **Table 2**, except for the detached breakwaters with K_t = 0.4 placed between x = −1.4 and − 0.5 km, and K_t = 0.8 for artificial reefs.

6.2 Results of the reproduction calculations

6.2.1 Change in contour lines

Figure 15 shows the calculation results between the first and fifth periods together with an additional expression of bathymetric changes relative to the bathymetry in 1947 (**Figure A2**). In the first period (**Figure 15(a)**), erosion concentrated around the Hino River mouth with gradual accretion west of x = 4 km because of the decreased Q_{in} of 6×10^4 m^3/year. Since the calculation was carried out using the expanded coordinates set on the shoreline in 1947, the triangular shoreline recession area shown in **Figure 15(a)** corresponds to the recession of the protruded shoreline of a river delta. The shoreline receded around the river mouth, whereas the contour lines advanced west of x = 5 km.

In the second period (**Figure 15(b)**), the seawall had been constructed between x = 0 and 1.5 km, although Q_{in} was the same (6×10^4 m^3/year) as that in the first period. Owing to the construction of the seawall, westward longshore sand transport was partially blocked at the protruded seawall, resulting in erosion immediately west of the structure with the accretion upcoast. In the third period, Q_{in} decreased from 6×10^4 to 4.7×10^4 m^3/year together with the construction of 12 DBs and Kaike fishing port breakwaters (**Figure 15(c)**). Soon after the construction of DBs, cuspate forelands were formed behind the DBs. Simultaneously, severe erosion occurred downcoast of Kaike fishing port located at x = 3 km because of the decrease in the westward longshore sand transport.

In the fourth period, although Q_{in} was the same (4.7×10^4 m^3/year) as that in the third period, new DBs were constructed between x = −3.5 and − 2.5 km, and between 3.5 and 7 km, and further seawall was constructed between x = −5 and 0 km, and between x = 3.5 and 13 km, as shown in **Figure 15(d)**. At this stage, land reclamation was carried out at the west end at the shoreline, and the shoreline length was decreased by 4 km, resulting in the advance of all the contour lines. Although the shoreline east of the structures was stabilized by the construction of many coastal structures, erosion is severe downcoast.

In the fifth period between 1995 and 2010 (**Figure 15(e)**), Q_{in} was kept constant at 4.7×10^4 m^3/year, the same as that in the fourth period. For the sand back pass, sand was excavated at a rate of 3×10^4 m^3/year at x = 13 km, and the same amount was supplied at x = 8 km. In addition to this, an L-shaped groin was constructed at x = 7 km, and an artificial reef and DBs were constructed between x = −5 and 0 km. The effect of blocking longshore sand transport by the land reclamation reached upcoast, and the contour lines between x = 13 and 7 km became straight.

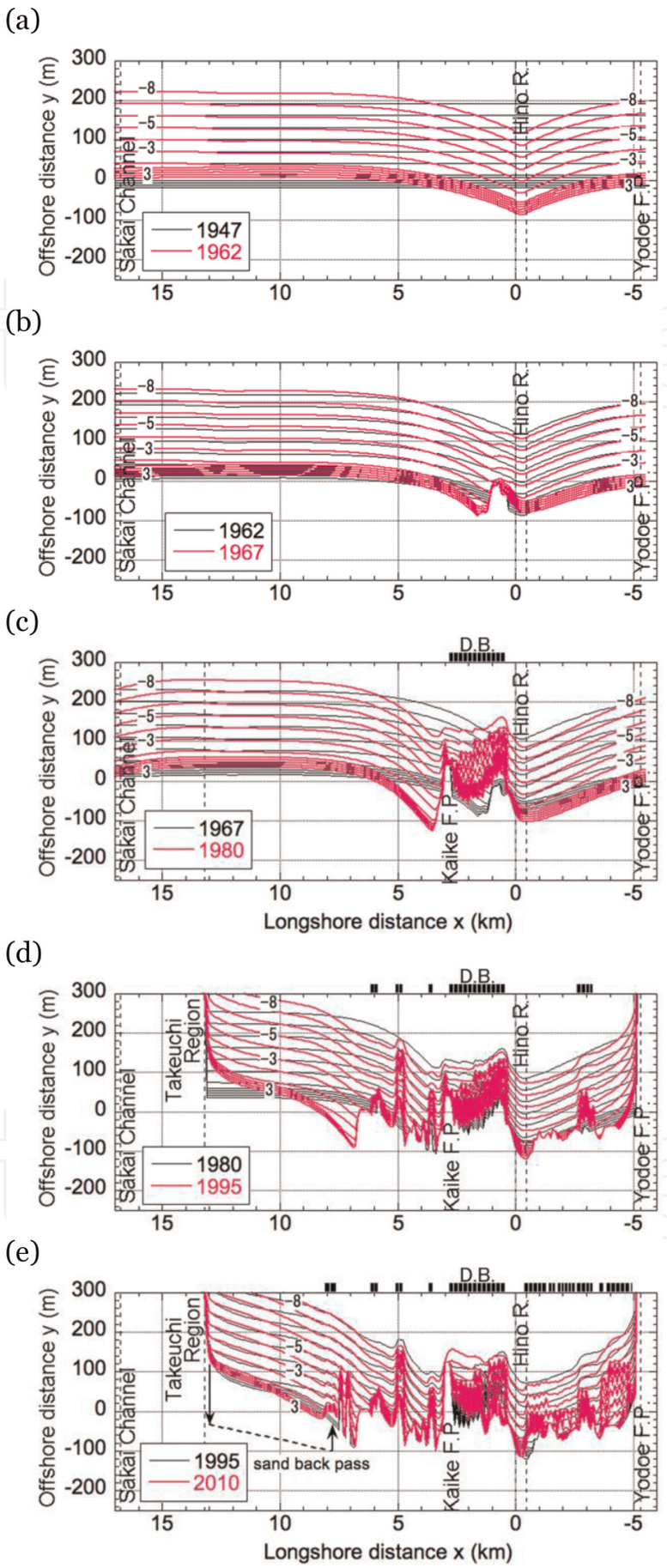

Figure 15.
Bathymetric changes between first period (1947–1967) and fifth period (1995–2010). (a) First period (1947–1962). (b) Second period (1962–1967). (c) Third period (1967–1980). (d) Fourth period (1980–1995). (e) Fifth period (1995–2010).

6.2.2 Depth changes

Figure 16 shows the measured and predicted shoreline changes between 1967 and 2007. The shoreline advance behind the DBs, downcoast shoreline recession, and the shoreline advance upcoast of the west boundary were in good agreement in the measured and predicted results. **Figure 17** shows the entire shoreline changes

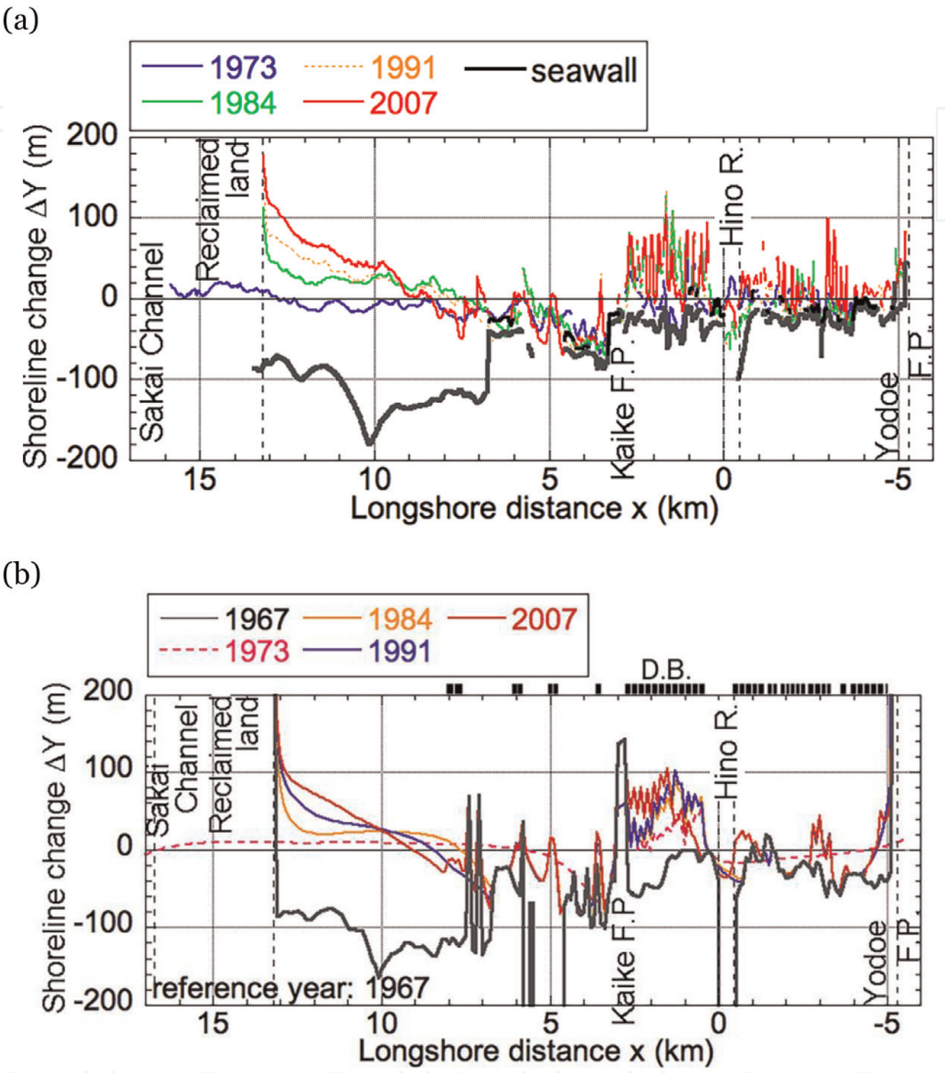

Figure 16.
Measured and predicted shoreline changes between 1967 and 2007. (a) Measured (1967–2007). (b) Calculated (1967–2007).

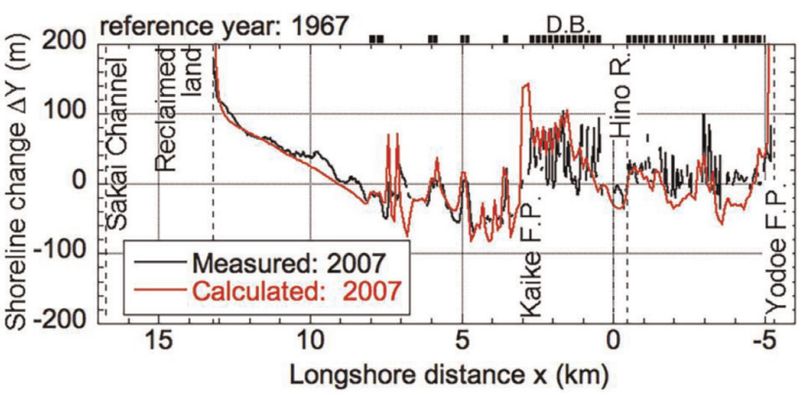

Figure 17.
Measured and predicted shoreline changes until 2007.

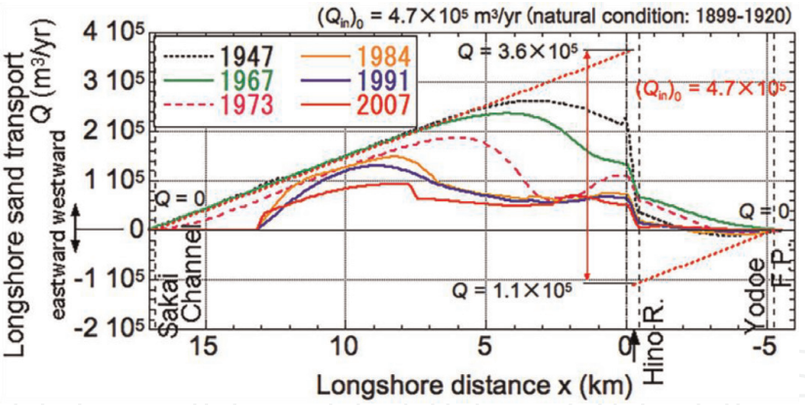

Figure 18.
Distribution of longshore sand transport rate.

until 2007 with reference to 1967. The predicted and measured shoreline changes agree well.

6.2.3 Comparison between measured and calculated shoreline changes

Figure 18 shows the distribution of longshore sand transport in the entire study area. Between 1899 and 1929, sand supplied from the Hino River was transported to both directions away from the river mouth with the westward and eastward transport of 3.6×10^5 and 1.1×10^5 m^3/year out of the entire sand supply of 4.7×10^5 m^3/year, respectively. With the decrease in sand supply from the Hino River, the longshore sand transport had decreased from the vicinity of the river mouth. In particular, the westward longshore sand transport markedly decreased after the construction of the DBs between 1967 and 1973 in the area between $x = 0$ and 3 km. East of the river mouth, eastward longshore sand transport at the initial stage reversed until 1967, and westward longshore sand transport began to occur after 1967.

7. Conclusions

The topographic changes of the Yumigahama Peninsula between 1899 and 2010 have been reproduced using the contour-line-change model considering the change in grain size of the seabed material. It was found that the beach changes of this peninsula were involved in the process leading to the reduction in the size of the Hino River delta, and strong erosion occurred around the river mouth. Because countermeasures were carried out from up the coast, sand was deposited up the coast of various structures with erosion down the coast. It was concluded that the contour-line-change model considering the change in grain size of the seabed material is a useful tool for predicting long-term topographic changes.

A. Appendix

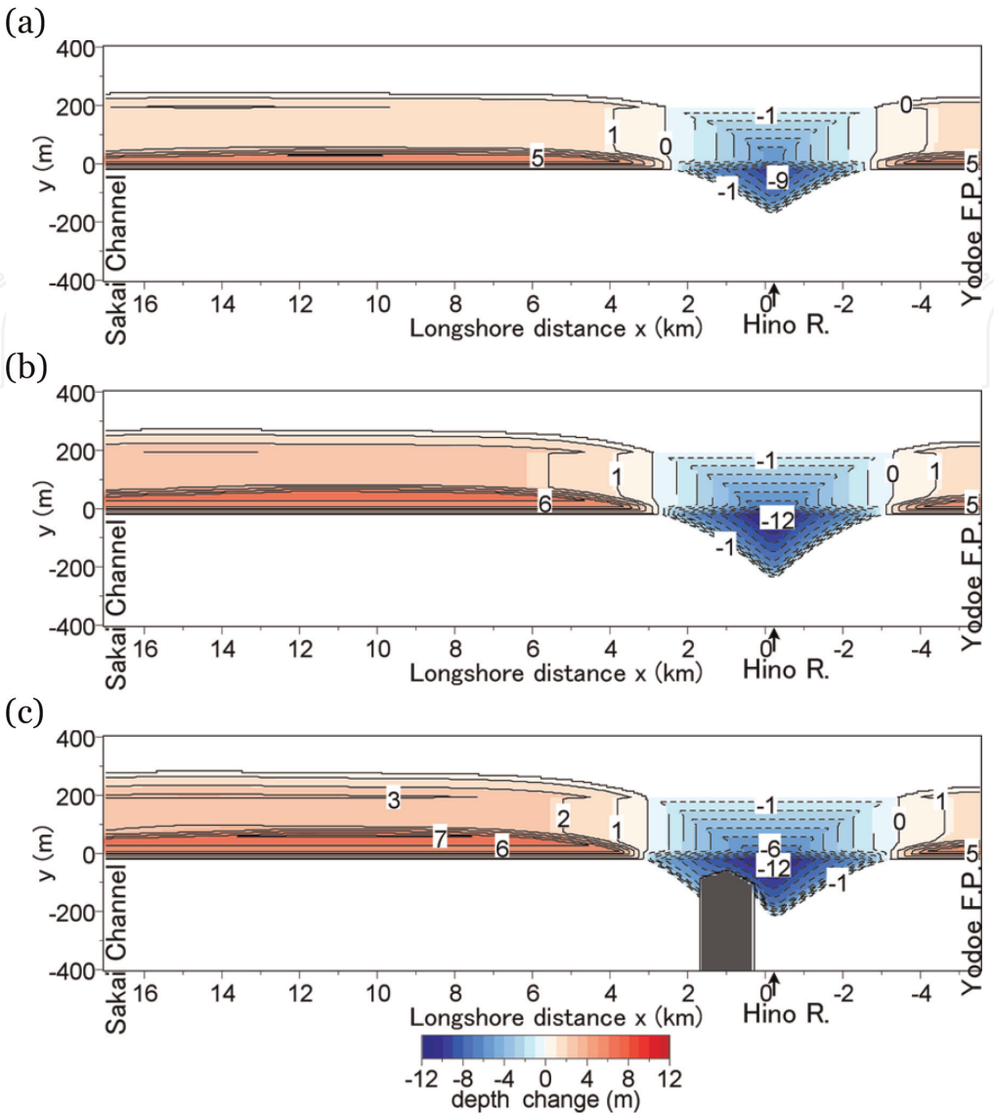

Figure A1.
Bathymetric changes until 1947, 1962, and 1967 with reference to bathymetry in 1920. (a) Bathymetric changes between 1920 and 1947. (b) Bathymetric changes between 1920 and 1962. (c) Bathymetric changes between 1920 and 1967.

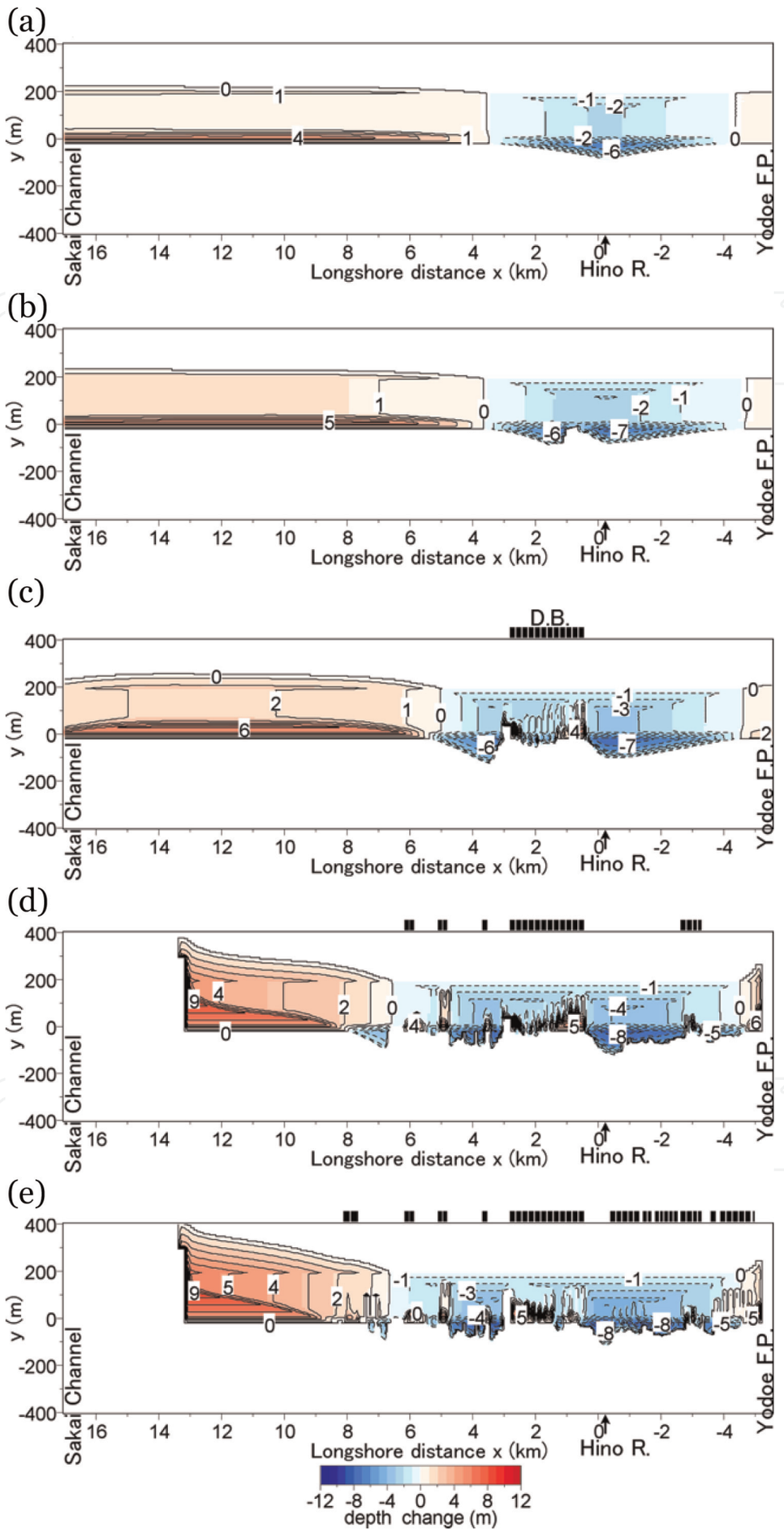

Figure A2.
Bathymetric changes with reference to bathymetry in 1947. (a) 1962. (b) 1967. (c) 1980. (d) 1995. (e) 2010.

Author details

Takaaki Uda[1], Shiho Miyahara[2*], Toshiro San-nami[2] and Masumi Serizawa[2]

1 Public Works Research Center, Tokyo, Japan

2 Coastal Engineering Laboratory Co., Ltd., Tokyo, Japan

*Address all correspondence to: miyahara11@gmail.com

IntechOpen

References

[1] Toyoshima O, Sadamichi N. Formation of tombolos and bathymetric changes on Kaike coast. In: Proceedings of the 21st Coastal Engineering Conference. JSCE; 1974. pp. 167-172 (in Japanese)

[2] Toyoshima O. Topographic changes owing to construction of detached breakwaters. In: Proceedings of the 24th Coastal Engineering Conference. JSCE; 1977. pp. 185-189 (in Japanese)

[3] Nishitani Y, Hayami M, Toyoshima O. Sand deposition effect of detached breakwater and bathymetric changes. In: Proceedings of the 28th Coastal Engineering Conference. JSCE; 1981. pp. 266-270 (in Japanese)

[4] Uda T. Beach Erosion in Japan. Tokyo: Sankaido Press; 1997. p. 442 (in Japanese)

[5] Uda T, Serizawa M, Miyahara S. Morphodynamic Model for Predicting Beach Changes Based on Bagnold's Concept and its Applications. London, UK: INTEC; 2018. p. 188. https://www.intechopen.com/books/morphodynamic-model-for-predicting-beach-changes-based-on-bagnold-s-concept-and-its-applications

[6] Bakker WT. The dynamics of a coast with a groyne system. In: Proceedings of the 11th Coastal Engineering Conference. ASCE; 1969. pp. 1001-1020

[7] Perlin M, Dean RG. A numerical model to simulate sediment transport in the vicinity of coastal structures. Miscellaneous Report, No. 83-10. Coastal Engineering Research Center, U.S. Army Corps of Engineers; 1983. p. 119

[8] Steetzel HJ, de Vroeg JH. Application of a multilayer approach for morphological modelling. In: Proceedings of the Coastal Sediments' 99. Vicksburg: ASCE; 1999. pp. 2206-2218

[9] Steetzel HJ, de Vroeg H, van Rijn LC, Stam JM. Long-term modelling of the Holland coast using a multi-layer model. In: Proceedings of the 27th International Conference on Coastal Engineering. Sydney, Australia: ASCE; 2000. pp. 2942-2955

[10] Dabees MA, Kamphuis JWNLINE. Efficient modeling of 3D beach change. In: Proceedings of the 27th International Conference on Coastal Engineering. Sydney, Australia: ASCE; 2000. pp. 2700-2713

[11] Hanson H, Larson M. Simulating coastal evolution using a new type N-line model. In: Proceedings of 27th International Conference on Coastal Engineering. Vicksburg: ASCE; 2000. pp. 2808-2821

[12] Hanson H, Aarninkhof S, Capobianco M, Jimenez JA, Larson M, Nicholls R, et al. Modelling coastal evolution on early to decadal time scales. Journal of Coastal Research. 2003;**19**:790-811

[13] Uda T, Serizawa M. Model for predicting topographic changes on coast composed of sand of mixed grain size and its applications (chap. 16). In: Angermann L, editor. Numerical Simulations—Examples and Applications in Computational Fluid Dynamics. Croatia: INTEC; 2010. pp. 327-358

[14] Uda T. Japan's Beach Erosion—Reality and Future Measures. 2nd ed. Singapore: World Scientific; 2017. p. 530

[15] Uda T, Yamagata H, Katoh K, Akamatsu N. Predictive model of three-dimensional development and deformation of a river mouth delta by applying contour line change model. In:

Proceedings of the 26th International Conference on Coastal Engineering. 1998. pp. 3138-3150

[16] Furuike K, Uda T, Serizawa M, San-Nami T, Ishikawa T. Model for predicting long-term beach changes originating from accretive features of a natural delta coast. In: Proceedings of the 5th International Conference on Asian and Pacific Coasts. Vol. 4. 2009. pp. 266-272

[17] Miyahara S, Uda T, Furuike K, Serizawa M, San-nami T, Ishikawa T. Effect of sand bypassing at Sakuma Dam in Tenryu River as a measure against erosion of Tenryu River delta coast. In: Proceedings of the 32nd ICCE, Sediment. 106. 2010. pp. 1-12. http://journals.tdl.org/ICCE/article/view/1049/pdf_165

[18] Miyahara S, Uda T, Ishikawa T, Furuike K, Serizawa M. Prediction of long-term topographic changes of Tenryu River delta associated with sand bypassing at dam in upper basin assuming no coastal facilities. In: Proceedings of the 6th International Conference, Asian and Pacific Coasts. 2011. pp. 216-223

[19] San-nami T, Furuike K, Uda T, Serizawa M. Formation of an arc-shaped accretive shoreline downcoast of sea cliffs and prediction of deformation. In: Proceeding of the Coastal Sediments. 2011. pp. 1243-1256

[20] San-nami T, Uda T, Ohashi N, Iwamoto H, Serizawa M, Ishikawa T, et al. Prediction of beach erosion caused by reduction of fluvial sand supply due to excess and mining and beach recovery after prohibition of mining. In: Proceedings of the 33rd International Conference on Coastal Engineering. Sediment. 61. 2012. pp. 1-11

[21] Kamphius JW, Davies MH, Narim RB, Sayao OJ. Calculation of littoral sand transport rate. Coastal Engineering. 1986;**10**:1-12

[22] Kumada T, Kobayashi A, Uda T, Serizawa M. Development of predictive model of shoreline and grain size changes. In: Proceedings of the Coastal Sediments. 2003. pp. 1-14

[23] Uda T, Kawano S. Development of a predictive model of contour line change due to waves. In: Proccedings of JSCE, No. 539/II-35. 1996. pp. 121-139 (in Japanese)

[24] Ozasa H, Brampton AH. Model for predicting the shoreline evolution of beaches backed by seawalls. Coastal Engineering. 1980;**4**:47-64

[25] Kraus NC. Field experiment on vertical mixing of sand in the surf zone. Sedimentary Petrology. 1985;**55**:3-14